Rheological properties of Triumfetta cordifolia gum solutions in the concentrated regime

Michèle Fanwa, Nicolas Hucher, Arnaud M.Y. Cheumani, Maurice Ndikontar, Catherine Malhiac, Michel Grisel

International Journal of Biological Macromolecules 279 (2024) 135335

Contents lists available at ScienceDirect

International Journal of Biological Macromolecules

journal homepage: www.elsevier.com/locate/ijbiomac

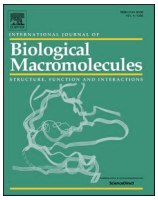

Rheological properties of *Triumfetta cordifolia* gum solutions in the concentrated regime

Michèle N. Fanwa [a,b,*], Nicolas Hucher [a], Arnaud M.Y. Cheumani [b], Maurice K. Ndikontar [b], Catherine Malhiac [a], Michel Grisel [a,**]

[a] Université Le Havre Normandie, Normandie Univ, URCOM UR 3221, F-76600 Le Havre, France
[b] Research Unit for Macromolecular Chemistry, Laboratory of Applied Inorganic Chemistry, Faculty of Science, University of Yaoundé I, P.O. Box 812, Yaoundé, Cameroon

ARTICLE INFO

Keywords:
Triumfetta Cordifolia gum
Rheology
Salt and pH effects

ABSTRACT

The polyelectrolyte gum from *Triumfetta cordifolia* stem bark has recently come to the fore for its remarkable potential as an emulsifier and stabilizer for aqueous formulations. This paper presents the rheological study of *T. cordifolia* gum aqueous solutions in the concentrated regime ($C > C^{**} = 0.14$ % *w*/w). To this end, both flow and oscillation tests were performed on *T. cordifolia* gum solutions at two distinct concentrations belonging to the concentrated regime: at 0.2 % *w*/w (close to C**) and at 0.7 % w/w (far above C**). The effect of temperature, pH and added salts (NaCl, $CaCl_2$ and $AlCl_3$) on gum viscoelastic parameters were investigated, revealing associative interactions. Under specific conditions, several remarkable and complex phenomena were observed, such as over-structuring induced by temperature, anti-thixotropy, gelation, syneresis and salting-out induced by salt addition. The charged structure of *T. cordifolia* gum (weak polyelectrolyte), the high divalent metal content and the presence of associative groups in its network were demonstrated as the major factors responsible for these phenomena. These findings form the basis for the structure-property relationships of *T. cordifolia* gum and may open up to further investigations for this gum of great potential in many fields of applications.

1. Introduction

T. cordifolia is a shrub belonging to the *Malvaceae* family [1] that is mainly found in humid parts of tropical Africa [2]. Several species of the same genus are also found in America, Asia and Oceania [3–5]. *T. cordifolia* grows fast, up to 2.5 m tall. It is cultivated either by cutting or by seed germination with a germination rate of 80 to 90 % [2]. The fruits with hooked hairs, are sometimes dispersed by animal fur, favoring its spread; interestingly, the shrub can be harvested several times during the year.

The gum, extracted from stem bark, is a polyelectrolyte made up of galacturonic and glucuronic acids, rhamnose and galactose (which are predominant), glucose, mannose, arabinose and xylose (in small proportions), with some carboxyl groups in the form of acetates [6–8]. It has a high mineral content, with a predominance of divalent metals (calcium and magnesium), followed by potassium [6,7]. *T. cordifolia* gum aqueous solutions have shown three main concentration regimes, with a propensity to form entanglements and relatively structured networks at moderate concentrations [6].

The leaves and mucilage from the stem bark are edible and used in traditional dishes and drinks, either as a main ingredient or as a thickener [9–11]. Moreover, *T. cordifolia* gum presents interesting properties as bio-emulsifier and stabilizer in oil-in-water emulsions, with a viscosifying contribution [12]. It also acts as a dough swelling enhancer in corn and sorghum doughnuts [7]. Such functional properties open up new prospects for the use of *T. cordifolia* gum in several industries such as food, cosmetics or pharmaceutics. As these industries are demanding and delicate, the introduction of a new ingredient requires meticulous analysis and mastery of its properties. The bio-sourced, biocompatible and biodegradable nature of *T. cordifolia* gum, its availability, the possibility of obtaining a high-purity gum and its good thermal stability [6] are all assets that meet the requirements of these industries. However, rheological properties are very important aspects to take into account and to study, since the quality and sensory response of formulated

* Correspondence to: M. N. Fanwa, Research Unit for Macromolecular Chemistry, Laboratory of Applied Inorganic Chemistry, Faculty of Science, University of Yaoundé I, P.O. Box 812, Yaoundé, Cameroon.
** Corresponding author.
E-mail addresses: michele.fanwa-nzokou@doct.univ-lehavre.fr (M.N. Fanwa), michel.grisel@univ-lehavre.fr (M. Grisel).

https://doi.org/10.1016/j.ijbiomac.2024.135335
Received 8 April 2024; Received in revised form 20 August 2024; Accepted 3 September 2024
Available online 4 September 2024

products depend on them. Furthermore, knowledge of the mechanisms governing the flow properties and viscoelastic response of relatively structured systems is always an asset for scientific advancement.

This work aimed at studying the rheological properties, namely flow and viscoelastic characteristics of *T. cordifolia* gum solutions in the concentrated regime, including the effect of pH, temperature and added salts. It should be mentioned that the effect of these variables on the viscosity of *T. cordifolia* gum had already been examined in a previous study, but this was limited to the case of dilute solutions and monovalent to divalent salts [7]. The present study goes a step further, focusing on the concentrated regime and evaluating not only viscosity, but all the gum's viscoelastic parameters, thus enabling a better appreciation of the influence of the variables studied. The choice to study the concentrated regime was motivated by the fact that, on the one hand, the interest to document such properties is of primary importance to implement the knowledge of the gum's properties; and on the other, the relatively low threshold of the concentrated regime of *T. cordifolia* gum with C** = 0.14 % *w*/w [6] makes this gum very interesting for industrial applications and suggests that most of these applications will involve the concentrated regime, hence the importance of studying it. In addition, it enriches the literature on polymer rheology in general, as the concentrated regime is an under-researched regime due to the difficulty of its implementation and handling. Another special feature of this work was to evaluate the effect of different harvesting periods on the rheological properties of the gum. To this end, both flow and oscillation tests were performed on a 0.7 % *w*/w *T. cordifolia* gum solution from three different batches as specified in Fanwa et al. [6] in order to assess the reproducibility of the rheological properties of the gum from different harvests. Then, the effects of pH, temperature and added salts including monovalent (NaCl), divalent ($CaCl_2$) and trivalent ($AlCl_3$) were investigated. In the first instance, salt addition was carried out while maintaining in the reaction medium the structural metals initially present in the gum. To assess the effect of added salt alone without the structural minerals, dialysis-controlled salt addition experiments were carried out on 0.2 % w/w gum solutions. For this second stage, the concentration was reduced to make the medium less viscous and ensure efficient ion exchange through the dialysis membrane. Thus, this work provides some rheological characteristics of both a near-C** concentrated regime (0.2 % *w*/w) and a far-C** concentrated regime (0.7 % w/w) of *T. cordifolia* gum, and establishes some relationships between the properties it exhibits in solutions and its structure.

2. Experimental

2.1. Materials and chemicals

T. cordifolia stems were collected in Yaoundé in the Centre region of Cameroon. The plant was identified by a botanist at the Cameroon National Herbarium using voucher specimen number 41920/HNC. Ultrapure water ($R > 18$ MΩ-cm, TOC < 1 ppb, bacteria <1 CFU/mL) was obtained from a Barnstead Easypure UV compact ultrapure water system (Thermo Scientific, Illkirch, France). Sodium chloride, anhydrous calcium chloride, and anhydrous aluminum chloride were purchased from Carlo Erba (Val-de-Reuil, France), Merck (Darmstadt, Germany) and Alfa Aesar (Kandel, Germany) respectively, while sodium hydroxide and hydrochloric acid were purchased from Fisher Scientific (Loughborough, United Kingdom). All chemicals were of reagent-grade and were used without further purification.

2.2. Sample preparation

The samples used in this study were prepared according to the method previously described in Fanwa et al. [6]. Briefly, *T. cordifolia* gum was extracted from fresh stem bark using cold distilled water at room temperature (25–30 °C). Stems were collected in a series of batches to assess the effect of variation in harvesting period on gum properties. In total, 3 series of collections were carried out over different periods: from January to April 2019 (batch 1), from December 2019 to January 2020 (batch 2) and from February to April 2022 (batch 3). For each collection, the stems were immediately transported to the laboratory, where they were subjected to a very rigorous and repeatable extraction protocol to obtain the crude extract, including washing, scraping and debarking followed by soaking in distilled water, kneading and pressing, vacuum filtration and gum precipitation using ethanol. Extracts obtained from a series of extractions during each harvesting season as defined above were pooled to form a single batch. Subsequently, each batch was dried, finely ground in a porcelain crucible, packaged in hermetically sealed polypropylene bottles and stored at 4 °C for further use.

On the other hand, gum stock solutions were prepared by first dissolving 400 ppm sodium azide (preservative) in ultra-pure water; the required amount of gum powder was then gradually added by sprinkling under mechanical agitation for 12 h to achieve complete dissolution, thus ensuring an efficient solubilization process. The solution was then centrifuged to remove insolubles and the true concentration was determined by calculating the dry matter content using thermal gravimetric analysis, as described in Fanwa et al. [6].

2.3. Salt addition

NaCl and $CaCl_2$ salts were added to a 0.7 % *w*/w *T. cordifolia* gum solution by introducing all the reagents (gum solution + salt solution) into a conical tube and vigorously vortexing the mixture. The case of the $AlCl_3$ salt was more complex, as rapid gel setting was observed at certain concentrations, giving rise to a heterogeneous mixture containing very elastic gel blocks, since the reaction with $AlCl_3$ took place only with the first polymer molecules with which it came into contact as gel setting was instantaneous. For this reason, a protocol allowing gradual addition of $AlCl_3$ solutions and a more turbulent agitation of the system was adapted (Fig. A.1 **in Appendix A**). Schematically, the gum solution was introduced into a flask containing magnetic bars, the stopper of which was pierced by a circular opening through which the saline solution was gradually added using a syringe, while the whole solution was being vortexed.

Prior to rheological analyses, all these solutions with added salts were degassed by low-speed centrifugation (at 100 *g* during 5 min for solutions containing NaCl or $CaCl_2$; 2 cycles at 2500 g during 5 min for gelled solutions containing $AlCl_3$) to avoid the concentration variations that vacuum degassing could cause. In the case of solutions/gels containing $AlCl_3$, analyses were carried out at least 48 h after preparation.

For dialysis-controlled salt addition, a 0.2 % *T. cordifolia* gum solution was introduced into a Spectrum™ 131,057 cellulose ester dialysis membrane with a MWCO (molecular weight cut-off) of 500 Da and a diameter of 24 mm. The gum solutions thus conditioned (~30 mL) were each introduced into a large volume (2000 mL) of dialyzing solution containing the salts at different concentrations (NaCl or $CaCl_2$ at 10^{-3}, 10^{-2}, 10^{-1} and 2×10^{-1} M or $AlCl_3$ at 10^{-4}, 5×10^{-4}, 10^{-3} and 5×10^{-3} M). The dialysis systems thus formed were kept under agitation in a room conditioned at 20 °C, while the conductivity of the medium was monitored. The dialysis process was stopped when the conductivity of the dialyzing solutions remained unchanged (and almost equal to the conductivity of the salts' stock solutions). In total, 2 cycles (dialyzing solutions being replaced once) lasting around 30 h were required.

2.4. Rheological characterization

Rheological measurements were carried out on *T. cordifolia* gum solutions using a DHR rheometer (TA instruments, New Castle, DE, USA), equipped with an aluminum cone–plate geometry (diameter 60 mm; angle 2.006; truncation gap 53 μm) and piloted by TRIOS software. Amplitude sweep tests were carried out at 1 Hz from 0.01 to 100 % while frequency sweep measurements were performed from 10^2 to 10^{-5} Hz at

1 % strain (belonging to the linear viscoelastic domain). Flow ramp tests were performed from 10^{-3} up to 10^{3} s^{-1}, during 300 s while flow sweep tests were conducted with a steady state sensing on the same shear rates range. All these tests were performed at 20 °C. Oscillation temperature ramps were carried out reversibly from 20 to 80 °C, then from 80 to 20 °C at the rate of 2 °C·min^{-1}. Temperature was controlled using a Peltier system with an accuracy of ±0.1 °C. Once loaded, the sample was kept at rest for 300 s (conditioning) before starting the experiment. A solvent trap was set up to prevent evaporation of the water contained in the sample, and also to ensure homogeneity of the sample temperature during measurements. For temperature ramps, the solvent trap was filled with low viscosity silicone oil. To ensure accurate results, a minimum of two replicates was carried out for each sampling.

3. Results and discussion

3.1. Flow and viscoelastic properties of concentrated T. cordifolia gum solutions

After delimiting the concentration regimes of *T. cordifolia* gum, which led to the identification of two critical concentrations C* = 0.03 % *w*/w and C** = 0.14 % w/w separating the dilute, semi-dilute and concentrated regimes [6], an in-depth rheological study of the concentrated regime was carried out. Indeed, the transition to the concentrated regime takes place at fairly low concentrations, and the concentrations used for various applications fall within this regime [12]. For this purpose, two concentrations of gum solutions, namely 0.2 % *w*/w (in the near-C** concentrated regime) and 0.7 % w/w (in the far-C** concentrated regime), were studied.

3.1.1. Flow behavior

T. cordifolia gum samples from different batches, collected during three different campaigns as specified in Fanwa et al. [6], were subjected to flow measurements. In all cases, viscosity curves exhibited a Newtonian plateau at low shear rates, followed by a shear-thinning or pseudoplastic domain as the shear rate increased (Fig. 1).

However, there are discrepancies between the different batches. As an illustration, the zero-shear viscosity η_0 values (calculated using the Carreau-Yasuda model which is the best fit among others for viscosity vs shear rate curves as given by the TRIOS™ software) for 0.7 % w/w gum solutions subjected to flow sweep tests are 124.6 ± 1.1; 91.3 ± 0.6 and 232.6 ± 5.3 Pa·s for batches 1, 2 and 3 respectively. In order to provide a reliable explanation for such discrepancies, a series of investigations was envisaged. The characterization of these three batches of *T. cordifolia* gum revealed a remarkable reproducibility in their properties (elemental composition, thermal properties, FT-IR spectra, intrinsic viscosity…) except marked discrepancies in some metal contents as indicated in Table 1 [6].

It is obvious that batch 2 contains considerably higher content of monovalent cations, namely potassium and sodium, the latter being more than fifty times higher than the others. As a consequence, excess sodium and potassium in solution, should markedly screen the polyelectrolyte charge effects in batch 2, which would adopt a less extended conformation, resulting in lower viscosity as the polymer chains align more easily with the flow direction. Batch 3 contains three times more iron than batches 1 and 2. Further tests are needed to determine whether this is divalent or trivalent iron, but in view of the very high viscosity of batch 3, it would more probably appear as trivalent iron, which forms inter-chain bridges by association with the carboxylate groups of uronic acids in which one iron atom can mobilize 3 carboxylates [13]. In such a case, it may involve more intermolecular interactions between polymer chains thus considerably enhancing the solution viscosity.

From the above considerations, as an anionic polyelectrolyte, the rheological properties of *T. cordifolia* gum solutions are dependent on metal ion content.

The effect of gum concentration on the flow properties of *T. cordifolia* gum solutions was also investigated. There is a significant gap between the viscosity curves obtained at 0.2 and 0.7 % *w*/w over the entire shear-rate range (Fig. 2).

These curves fit the Carreau-Yasuda model (**Eq. 1**), the best fit among others for viscosity vs shear rate curves as given by the TRIOS software

$$\eta = \eta_\infty + (\eta_0 - \eta_\infty)[1 + (\lambda\gamma)^a]^{\frac{n-1}{a}} \quad (1)$$

where η_0 is the zero-shear viscosity, η_∞ the infinite viscosity, λ the consistency (characteristic time), n the rate index or power law index which measures the shear dependance ($n < 1$ for shear-thinning, $n = 1$ for Newtonian and $n > 1$ for shear-thickening fluids), and a reflects the transition index describing the transition between Newtonian plateau and power law region.

The Newtonian viscosity sharply increases from 22.3 ± 0.7 to 232.6 ± 5.3 Pa·s when the gum concentration is increased from 0.2 to 0.7 % (*w*/w). Such an increase in viscosity with gum concentration is evidence of increased entanglements in the system. The more entanglements there are within the system, the more pronounced the disentanglement during shearing as confirmed by the power law index measuring the degree of

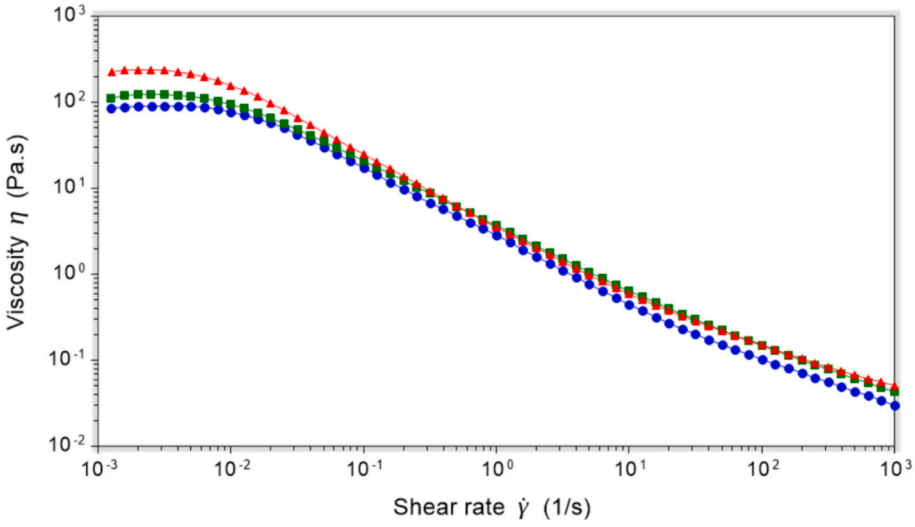

Fig. 1. Flow sweep curves of 0.7 % *w*/w *T. cordifolia* gum solutions at 20 °C: batch 1 (■green squares), batch 2 (●blue circles) and batch 3 (▲red triangles). (For interpretation of the references to colour in this figure legend, the reader is referred to the web version of this article.)

Table 1
Mineral content of different batches of *T. cordifolia* gum.

Batch	Mineral content (mg/g)						
	Ca	Fe	K	Mg	Mn	Na	Zn
Batch 1	23.44 ± 1.77	0.03 ± 0.01	1.20 ± 0.08	10.65 ± 0.83	0.56 ± 0.04	0.08 ± 0.02	0.06 ± 0.01
Batch 2	21.61 ± 1.70	0.03 ± 0.01	**3.39 ± 0.17**	10.24 ± 0.84	0.53 ± 0.03	**4.79 ± 0.17**	0.05 ± 0.01
Batch 3	24.59 ± 1.42	**0.10 ± 0.01**	1.64 ± 0.02	10.75 ± 0.57	0.43 ± 0.01	0.05 ± 0.01	0.07 ± 0.01

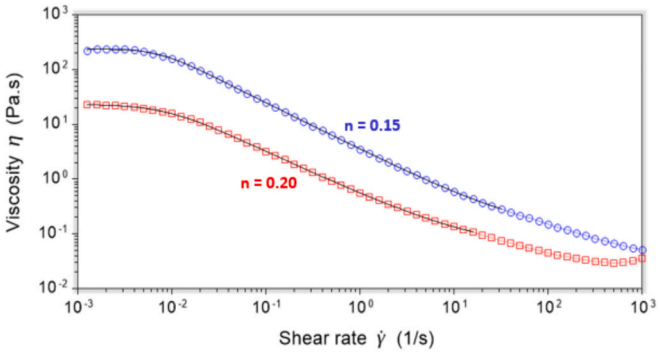

Fig. 2. Flow sweep curves of 0.2 % w/w (□red squares) and 0.7 % w/w (○blue circles) *T. cordifolia* gum solutions at 20 °C (batch 3). Black lines represent modeling curves. (For interpretation of the references to colour in this figure legend, the reader is referred to the web version of this article.)

shear-thinning which decreases from 0.21 ± 0.01 for the 0.2 % w/w gum solution to 0.13 ± 0.02 for the 0.7 % w/w solution.

At a later stage, *T. cordifolia* gum solutions were subjected to different shear modes to assess the effect of the nature of the shear on the flow properties. There are significant differences between zero-shear viscosities obtained when the gum samples were subjected to a continuous flow ramp (in which the sample acquires an instantaneous viscosity at each applied shear rate) and when they were subjected to a steady-state flow sweep (in which the sample is sheared at a constant rate until equilibrium is reached, before moving on to the next shear rate). As an illustration, the zero-shear viscosity of 0.7 % *w*/w *T. cordifolia* gum solutions under increasing shearing (from low to high shear rates) changes from 31.8 ± 0.2 Pa·s and 63.9 ± 1.9 Pa·s under continuous flow ramp to 91.3 ± 0.6 Pa·s and 232.6 ± 5.3 Pa·s under steady-state flow (maximum equilibrium time: 100 s; sample period: 10 s) for batches 2 and 3 respectively.

Moreover, in the case of steady-state flow, the viscosity obtained is highly dependent on the pre-defined steady-state parameters. For example, increasing steady-state parameter values from A (maximum equilibrium time: 100 s; sample period: 10 s) to B (maximum equilibrium time: 500 s; sample period: 100 s) on a 0.7 % w/w gum solution (batch 3) induced a sharp increase in viscosity from 232.6 Pa·s to 523.8 Pa·s; suggesting that the flow behavior of *T. cordifolia* gum solutions is strongly dependent on their shear history. Table 2 clearly summarizes the effects of gum concentration and shear mode /shear history on batch 3.

Table 2
Newtonian viscosity of *T. cordifolia* gum solutions (batch 3) at 20 °C as a function of concentration and shear mode.

Test	C (% w/w)	Batch 3
Flow ramp	0.2	5.1 ± 0.4
(10^{-3} s^{-1} to 10^{3} s^{-1}; 300 s)	0.7	63.9 ± 1.9
Flow sweep	0.2	22.3 ± 0.7
(10^{-3} s^{-1} to 10^{3} s^{-1}; steady state sensing-max. eq. time: 100 s; sample period: 10 s)	0.7	232.6 ± 5.3
Flow sweep	0.2	43.4 ± 1.3
(10^{-3} s^{-1} to 10^{3} s^{-1}; steady state sensing-max. eq. time: 500 s; sample period: 100 s)	0.7	523.8

To better assess this shear history dependence, reversible flow sweep measurements were carried out on both 0.2 and 0.7 % *T. cordifolia* gum solutions by applying increasing shear rates from 10^{-3} to 10^{3} s^{-1}, then decreasing shear rates from 10^{3} to 10^{-3} s^{-1}. Results are shown in Fig. 3.

Unlike the Newtonian plateau that characterizes the upward curves at low shear rates, the downward curves are rather characterized by an ever-increasing viscosity as the shear rate approaches zero. Once again, there is an effect of gum concentration: for 0.7 % solutions, the shift between up and down curves is only pronounced at low shear rates (~10^{-3} - 10^{-2} s^{-1}), then disappears at intermediate shear rates, and again forms a less pronounced loop at high shear rates (~10–10^{3} s^{-1}) (Fig. 3b), while for 0.2 % solutions, an anticlockwise hysteresis loop forms over the entire range of applied shear rates as shown in Fig. 3a, suggesting a structuring under shear. However, further analysis is needed to better understand and explain such behavior.

3.1.2. Viscoelastic response to amplitude and frequency sweep tests

First, amplitude sweep measurements were carried out on *T. cordifolia* gum solutions to determine the linear viscoelastic region (LVER) and assess the viscoelastic parameters of the gum on this linear domain. The three batches were tested at the concentration of 0.7 % *w*/w and the effect of gum concentration was assessed on batch 3 by additionally testing a 0.2 % w/w solution. Fig. 4 shows an example of amplitude sweep curve, while the viscoelastic parameters obtained from different samples are summarized in Table 3 (the LVER limit was calculated with a tolerance of 5 % ie ~5 % drop in the storage modulus from the average of the plateau).

Overall, *T. cordifolia* gum solutions exhibit an extended LVER (>30 %), with the elastic modulus G′ much greater than the viscous modulus G″, showing a weak gel behavior (tan δ = 0.2–0.5). As previously observed with flow measurements, batch 3 is more structured than the two others, with a higher G′ and a lower tan δ, suggesting that the elastic network in batch 3 is a little stiffer than in other batches.

Further, the frequency-dependence of the viscoelastic properties was investigated through frequency sweep measurements. Results showed that the viscoelastic response of *T. cordifolia* gum solutions towards frequency is concentration-dependent (Fig. 5).

For 0.2 % *w*/w solutions, both moduli are very close and highly dependent on frequency as usually found for lightly entangled polymers [14–16]. The curves display a modulus crossover **Co**, delimiting the viscous regime (G″ > G′) from the elastic regime (G′ > G″). In contrast, for 0.7 % w/w *T. cordifolia* gum solutions in the elastic regime, the elastic modulus is much greater than the viscous modulus. G' becomes less frequency-dependent and tends to form a plateau, evidence that there are more entanglements within the system [17,18] which is confirmed by a lower tan δ.

The inverse of the frequency at the crossover **Co** (0.048 ± 0.001 Pa; $2.6 \times 10^{-4} \pm 5.8 \times 10^{-6}$ Hz) between the elastic and viscous regimes is the relaxation time [19–21]. As this crossover occurs at very low frequencies ($f_{Co} = 2.6 \times 10^{-4} \pm 5.8 \times 10^{-6}$ Hz), it implies high relaxation times (τ = 3922 ± 89 s). Such a long relaxation time explains the formation of the anti-thixotropic hysteresis loop between the upward and downward flow curves observed in the previous section (Fig. 3).

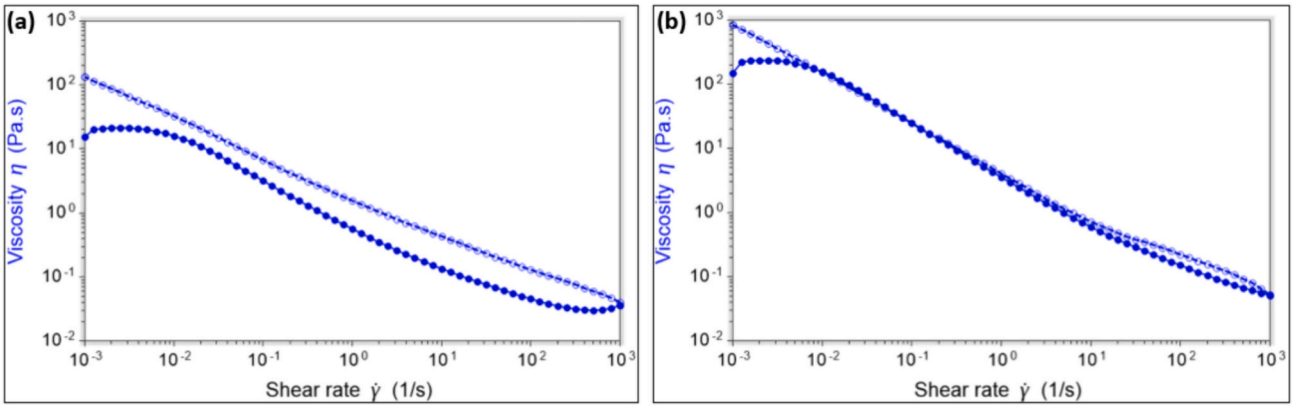

Fig. 3. Hysteresis between up (●filled symbol) and down (○empty symbols) flow sweep curves (maximum equilibrium time: 100 s; sample period: 10 s) of 0.2 % *w*/w **(a)** and 0.7 % w/w **(b)** *T. cordifolia* gum solutions at 20 °C.

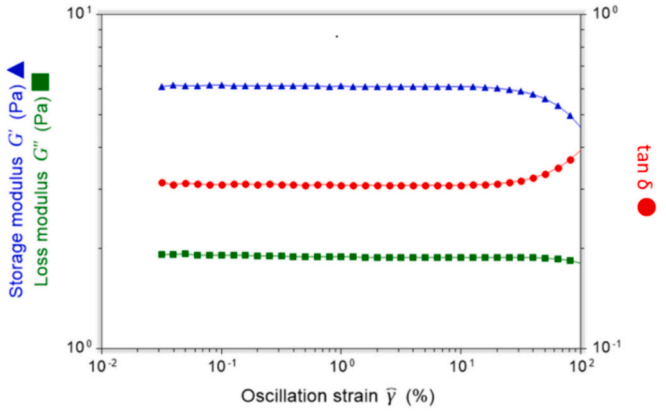

Fig. 4. Amplitude sweep curve of a 0.7 % *w*/w *T. cordifolia* gum solution at 20 °C.

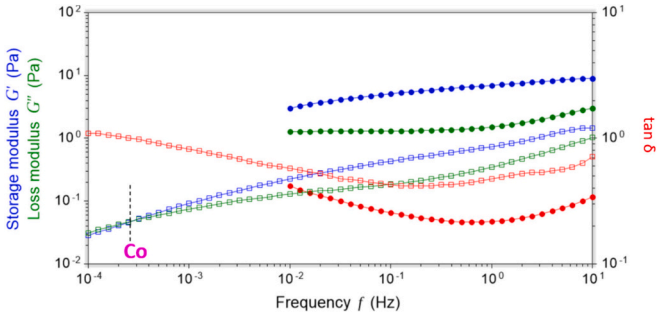

Fig. 5. Frequency dependence of the viscoelastic parameters of a 0.2 % *w*/w (□empty squares) and a 0.7 % w/w (●filled circles) *T. cordifolia* gum solutions.

Table 3
Viscoelastic parameters of *T. cordifolia* gum solutions from different batches at 20 °C.

C (% *w*/w)	Parameter	Batch 1	Batch 2	Batch 3
0.2	G′ (Pa)	n.t.	n.t.	0.86 ± 0.06
	G″ (Pa)			0.39 ± 0.02
	tan δ			0.45 ± 0.01
0.7	G′ (Pa)	6.08 ± 0.02	4.5 ± 0.2	7.22 ± 0.03
	G″ (Pa)	1.88 ± 0.01	1.24 ± 0.03	1.64 ± 0.01
	tan δ	0.309 ± 0.001	0.274 ± 0.008	0.228 ± 0.001
	LVER limit (%)	~40	~45	~33

n.t. = not tested.

3.1.3. Impact of shear on the viscoelastic behavior

Previous subsections have revealed, on the one hand shear-induced structuring of *T. cordifolia* gum, particularly for the 0.2 % *w*/w solution, marked by the formation of an anticlockwise hysteresis loop when a reversible flow sweep is applied (Section 3.1.1) and long relaxation times for these solutions on the other hand (Section 3.1.2). To better assess the magnitude of such structuring phenomenon, a 4-step test combining both flow and oscillation measurements was carried out as follows: (1) oscillation amplitude sweep on the gum solution at rest; (2) upward and downward flow sweep (maximum equilibrium time: 500 s; sample period: 100 s); (3) 300 s conditioning; (4) oscillation amplitude sweep on the sheared gum. Results are presented in Fig. 6.

The comparison of the viscoelastic parameters before and after the reversible sweep revealed a 10-fold increase in the elastic modulus

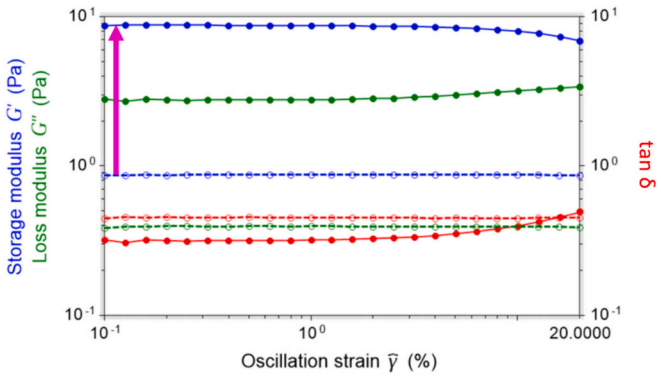

Fig. 6. Illustration of shear-induced structuring of a 0.2 % *w*/w *T. cordifolia* gum solution (at 20 °C) with a tenfold increase in elastic modulus: initial moduli in open symbols○ and broken lines–; moduli after reversible flow sweep (from 10^{-3} to 10^{3} s^{-1} then from 10^{3} to 10^{3} s^{-1}; maximum equilibrium time: 500 s; sample period: 100 s) and 5 min conditioning in filled symbols● and solid lines–.

under shear, despite a relaxation time of 5 min, clearly too short to recover the original structure; confirming the structure build-up of the gum under shear.

Overall, the above considerations suggest that *T. cordifolia* gum probably exhibits an anti-thixotropic behavior. Such anti-thixotropy can be explained by the following mechanism: shear induces a reorganization of the polyelectrolyte chains, which align themselves in the direction of flow [22], while unfolding their associative groups [-OH; $-COO^{-}$; $-O(C{=}O)CH_3$…] which then form intermolecular associations, possibly through the formation of hydrogen bonding or ionic bridges (between

oppositely charged groups), or through hydrophobic interactions (if there are sufficient hydrophobic acetate groups in the system). These intermolecular associations give rise to a more structured network whose resistance to creep leads to an increase in viscosity, as observed. Wee et al. [23] also found an anti-thixotropic behavior at certain shear rates in 5 % w/w solutions of the mucilage from *Cyathea medullaris* (known as mamaku gum) which they attributed to the formation of shear-induced intermolecular association structures most likely through hydrogen bonding as observed in other polymers [24–26].

As reversibility (recovery of the original viscosity at rest) is a condition for the anti-thixotropy phenomenon [27–29], this aspect was verified in the case of 0.7 % solutions by carrying out several series of peak-hold measurements alternating with rest periods. This involved subjecting the sample to constant shear, namely at 10^{-2} and 10^{3} s^{-1} (shear rates included in the antithixotropic zones observed in Fig. 3), while following the evolution of viscosity as a function of time, then leaving the sample at rest to appreciate relaxation before putting it back under constant shear again. The rheograms obtained from these alternating measurements were grouped together on a continuous time scale (Fig. 7).

It appears that the viscosity of *T. cordifolia* gum solution under constant shear increases as a function of time, which means that shear causes a progressive structuring of the gum over time. This effect is more pronounced at a shear rate of 10^{-2} s^{-1} and begins to stabilize at around 300 s. When shear is removed, the sample at rest undergoes perfect relaxation and returns to its initial viscosity. This cycle is repeated as many times as the test is repeated, which tends to confirm antithixotropy. This test also suggests that 0.7 % *T. cordifolia* gum solutions would have much shorter relaxation times than 0.2 % solutions.

However, as antithixotropy is a complex and poorly documented phenomenon, it would be important to carry out additional analyses, in particular the measurement of relaxation times for 0.7 % gum solutions and the combination of peak-hold and oscillation time sweep tests, in order to confirm and better understand this phenomenon in *T. cordifolia* gum solutions.

3.2. Behavior of T. cordifolia gum solutions subjected to different external conditions

3.2.1. Effect of temperature

Both 0.2 and 0.7 % *w*/w *T. cordifolia* gum solutions were subjected to an oscillation temperature ramp from 20 to 80 °C and from 80 to 20 °C while their mechanical properties were recorded. It follows that the viscoelastic response of concentrated *T. cordifolia* gum solutions to temperature varies with concentration (Fig. 8).

In both cases, no phase transition occurs and the weak-gel character is maintained over the entire temperature range, as the storage modulus remains higher than the loss modulus (tan δ = 0.24–0.46), and there is no modulus crossover during ramps.

At 0.7 % w/w gum concentration, solutions exhibit an integral thermo-reversible behavior. As the temperature varies, there is a little change in viscoelastic parameters, with a slight de-structuring on heating and perfect recovery on cooling (Fig. 8a). In this case, the entropic contribution governs the stiffness of the system which is highly entangled and behaves like rubber bands in which cross-links provide a network which is stretched upon stress (increase in temperature), but entropic forces favor the retraction of the system which return to its original state as the temperature is decreased (stress removed) [30,31]. Here, the space occupancy expressed as the coil overlap parameter C[η] is important and chains are very tightly packed, which limits Brownian motion.

On the other hand, at 0.2 % *w*/w gum concentration, solutions exhibit thermal stability on heating, with the viscoelastic parameters G′, G″ and tan δ remaining almost temperature-independent during the ramp; while on cooling, there is an over-structuring of the system, in particular, a strengthening of the elastic properties (increase in the elastic contribution G′), the viscous parameter remaining unchanged (Fig. 8b). Although the concentrations are different, the perfect reversibility of the viscous modulus is in agreement with the work of Saidou [7], who demonstrated perfect reversibility of the absolute viscosity of a 0.012 % (*w*/w) *T. cordifolia* gum solution subjected to heating from 10 to 80 °C and then cooling from 80 to 10 °C. Averaging the first 10 points of the heating curve and the last 10 points of the cooling curve over three replicates clearly shows that the system has moved from an initial state A (G′ = 0.9 ± 0.02 Pa; G″ = 0.4 ± 0.002 Pa; tan δ = 0.44 ± 0.01) to a more structured state B (G′ = 1.2 ± 0.05 Pa; G″ = 0.4 ± 0.02 Pa; tan δ = 0.34 ± 0.002). These observations suggest that *T. cordifolia* gum has a pronounced associative character. Indeed, as the chains are weakly entangled and the space occupancy is relatively low, increasing temperature induces thermal agitation of the molecules in the gum solutions, expressed as Brownian motion which, despite its low magnitude due to entanglements, allows random unfolding of associative groups

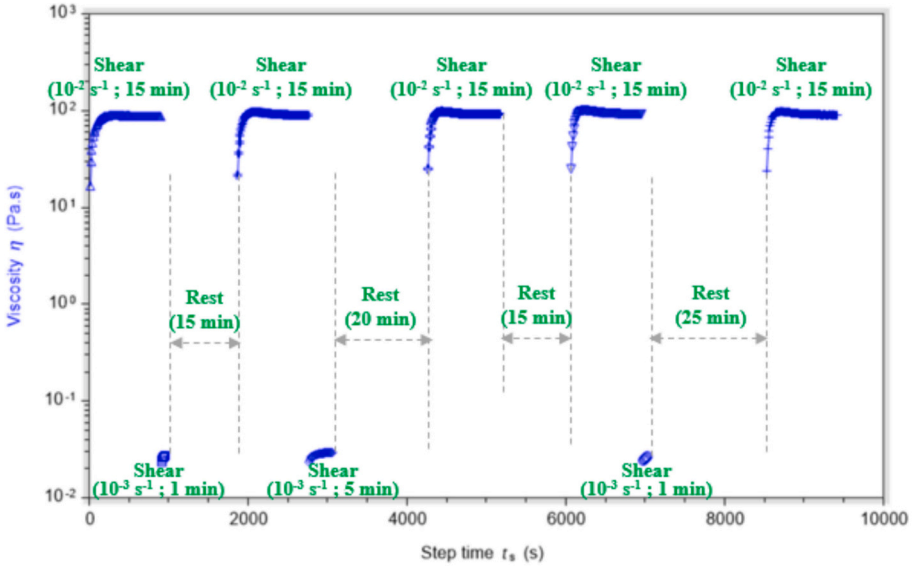

Fig. 7. Viscosity vs. time curves for a 0.7 % aqueous solution of *T. cordifolia* (batch 2) preconditioned at 20 °C for 5 min and subjected to peak-hold tests alternating with rest phases.

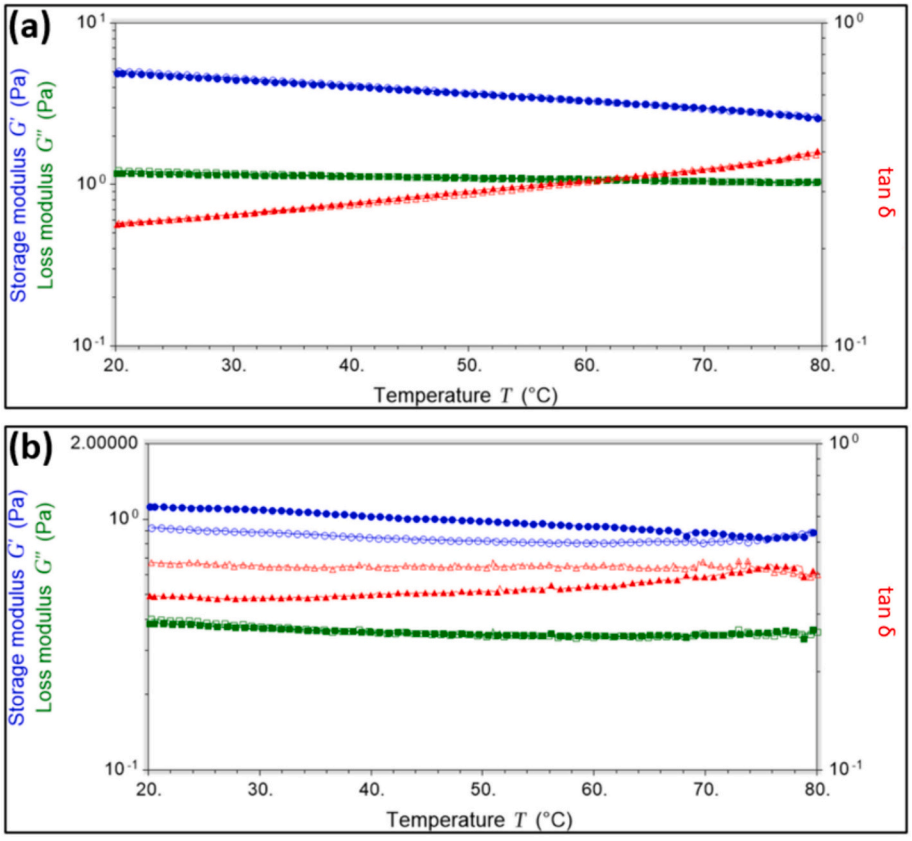

Fig. 8. Temperature-dependence of the viscoelastic moduli of 0.7 % w/w **(a)** and 0.2 % w/w **(b)** *T. cordifolia* gum solutions: upward curves in open symbols○△□ and downward curves in filled symbols●▲■.

[32]. Subsequently, the unfolded associative groups establish intermolecular bridges during cooling, giving rise to a more structured system than the initial one as shown in Fig. 8b. This associative behavior seems to confirm the anti-thixotropy phenomenon mentioned earlier for 0.2 % *w*/w gum solutions, as shown in Figs. 3 and 7, in which the unfolding of associative groups is rather induced by shear. Thus, 0.2 % w/w *T. cordifolia* gum solutions exhibit both shear- and temperature-induced associations. It would be interesting to carry out complementary measurements using the time-temperature superposition (TTS) principle, in order to better assess the temperature-dependence of the mechanical properties of *T. cordifolia* gum.

3.2.2. *Effect of pH*

As *T. cordifolia* gum is a weak acidic polyelectrolyte bearing carboxylic acid functions of uronic acids, which are probably present both in acid and base forms, it is conceivable that its properties in solution are highly dependent on the pH of the medium (since a pH change modify the balance between acid and base forms). Hence, rheological properties of a 0.7 % *T. cordifolia* gum solution with an acidic initial pH of 5.9 were monitored as a function of pH (Fig. 9a), the pH being controlled by increments of HCl or NaOH solutions (from stock solutions of 10^{-1} M HCl; 1.6×10^{-2} M and 1 M NaOH).

Fig. 9a shows that viscosity peaks at intermediate pH values and decreases on both sides, i.e. at lower and higher pH values. The same trend was reported by Saidou [7] for a very dilute gum solution (0.012 %) investigated over a more complete pH range (from 2 to 12). The drop in viscosity for lower and higher pH could be explained by polymer collapse due to fluctuations in the acid-base equilibrium of the carboxylic acid groups. Indeed, weak polyacids are uncharged at low pH and fully charged at high pH [33]. On the one hand, as the polyelectrolyte is no longer charged at low pH, electrostatic repulsion ceases, and intra- and intermolecular hydrogen bonding are established, causing the

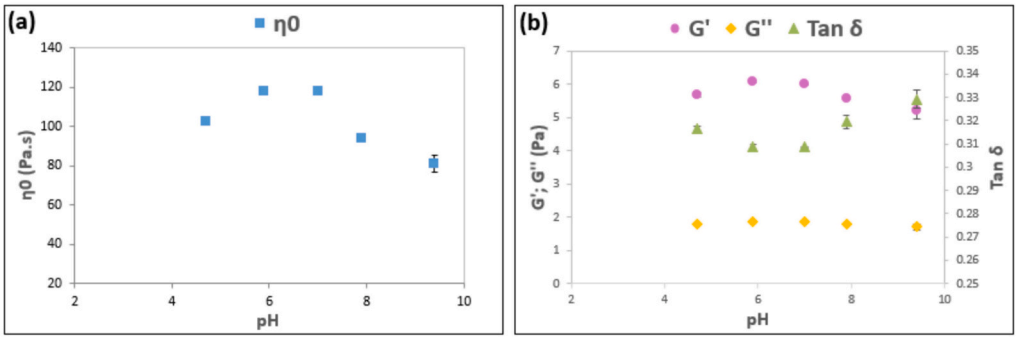

Fig. 9. Newtonian viscosity **(a)** and viscoelastic moduli **(b)** of a 0.7 % w/w *T. cordifolia* gum solution as a function of pH.

polymer to collapse, hence the observed drop in viscosity. On the other hand, when the polyelectrolyte becomes fully charged at higher pH values, the predominant divalent cations (Table 1**)** condense in priority on certain charged sites, inducing a charge inversion. Similarly, Na^+ ions from the added base (NaOH) condense on other sites and neutralize them, thus reducing part of the electrostatic tension within the system. Subsequently, electrostatic attraction between the positively- and negatively-charged sites will further accentuate the collapse of the polymer, leading to a decrease in viscosity. Furthermore, Fig. 9b shows that viscous modulus is virtually unaffected by pH variation over the entire measurement range; only elastic modulus and tan d are affected, but as with viscosity, the effect tends to be significant only towards the extremes.

Overall, the fact that viscoelastic parameters of *T. cordifolia* gum solutions hardly varies in the intermediate pH range is an advantage for potential applications in the food, cosmetics or pharmaceutical industries, since corresponding formulations are generally found in this intermediate pH range [34,35]. As an illustration, the 80/20 (*w*/w) oil-in-water emulsions formulated in a previous study with cocoglyceride oil using 0.2 % (w/w) *T. cordifolia* gum as emulsifier, texturizer and stabilizer, without the need for pH adjustment, showed a constant viscosity throughout the 31-day monitoring period [12]; pH varying only slightly between 4.4 and 4.8, a pH range that respects the acid-base balance of the skin which is moderately acidic [36,37].

3.2.3. *Effect of added salts*

It is known that the dissociation of weak acids is partial, and both acid and base forms coexist in the medium. The pK_a values obtained by Kohn and Kovac [38] for glucuronic and galacturonic acids at 20 °C are 3.28 and 3.51 respectively. As the pH of *T. cordifolia* gum solutions is close to 6 (i.e. $pH > pK_a + 2$), the basic form is preponderant (about 100 times more than the acid form), meaning that most structural units bearing uronic acid groups are dissociated in the form of uronates associated with the minerals found in the gum. Unlike the dilute regime, in which counter-ions would be mobile in solution, the decrease in entropy in the concentrated regime gives rise to counter-ion condensation. There is therefore a high proportion of counter-ions which are condensed on the polyelectrolyte and some counter-ions free to move in solution, as predicted by the Oosawa-Manning model [39]. Thus, the nature and density of charges in the condensation sphere, and hence the behavior of the polyelectrolyte, are likely to be strongly impacted in the presence of other ionic species, hence the interest in studying the effect of salts, in particular the effects of the nature and the concentration of salts.

To this end, three types of salts of different valencies, namely monovalent (NaCl), divalent ($CaCl_2$) and trivalent ($AlCl_3$), were added to the polyelectrolyte at different concentrations. In a first step, the salt solutions were directly introduced into the gum solutions, while in a second step, gum solutions were dialyzed against salt solutions.

3.2.3.1. Direct salt addition. The various salts were added directly to a 0.7 % *T. cordifolia* gum solution at different concentrations (10^{-1}, 2×10^{-1}, 3×10^{-1} & 4×10^{-1} M for NaCl; 10^{-1}, 2×10^{-1}, 3×10^{-1}, 4×10^{-1} & 6×10^{-1} M for $CaCl_2$; 10^{-3}, 2×10^{-3}, 3×10^{-3}, 3.5×10^{-3}, 4×10^{-3} & 5×10^{-3} M for $AlCl_3$) and the rheological properties were evaluated. Fig. 10 shows the evolution of the gum's viscoelastic parameters as a function of salt concentration.

In the case of the monovalent salt, viscosity and storage modulus

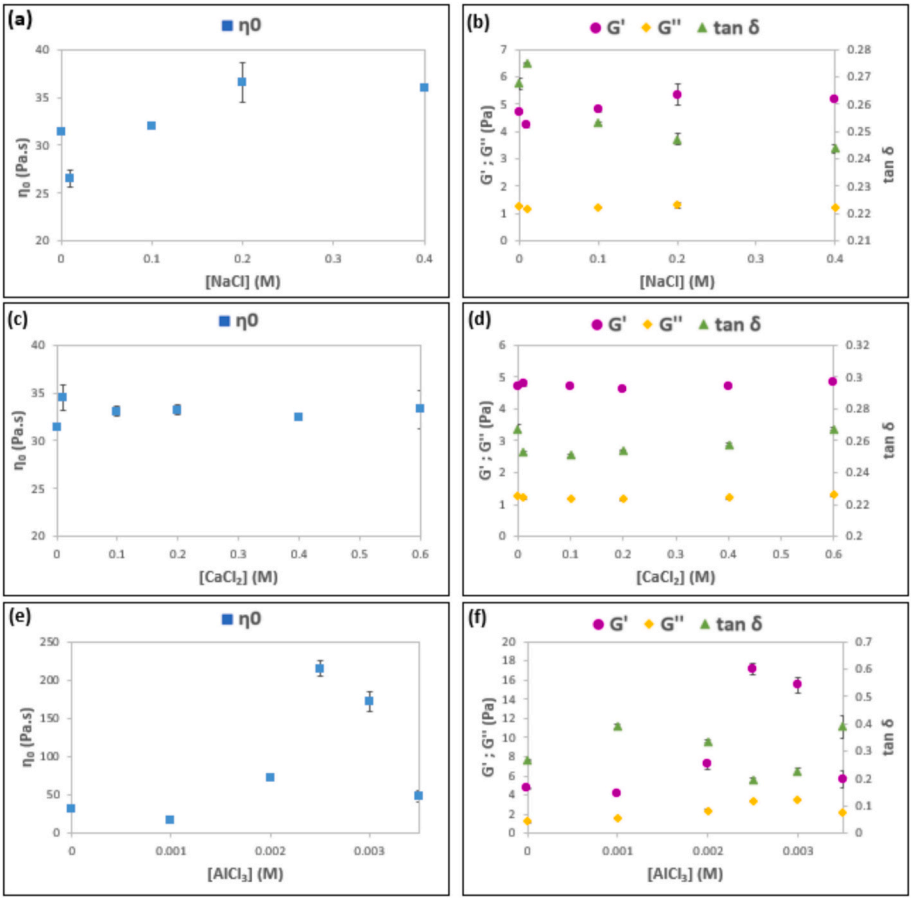

Fig. 10. Evolution of Newtonian viscosity and viscoelastic moduli of a 0.7 % *T. cordifolia* gum solution as a function of NaCl (**a & b**), $CaCl_2$ (**c & d**) and $AlCl_3$ (**e & f**) concentrations.

initially decrease, then increase again when sufficient salt is added (Fig. 10a & b) while with the divalent salt, there is only a moderate increase in viscosity, which then stabilizes and stops changing at around 0.1 M $CaCl_2$ (Fig. 10c). The case of the trivalent salt is more complex. First, there is a drop in viscosity at very low concentrations (10^{-3} M); then, an exponential increase in viscosity and elastic modulus is observed (Fig. 10e & f), with gel formation around 2.5×10^{-3} M (tan δ = 0.19 ± 0.009). Subsequently, a drastic drop in viscosity occurs, followed by phase separation (precipitation) as the salt concentration is further increased. *Re*-solubilization was not observed when excess $AlCl_3$ was added. These variations in the behavior of the polyelectrolyte *T. cordifolia* gum result from the fluctuations in the condensation sphere as different cations are added. Fig. 11 summarizes the main phenomena occurring in each case.

The mechanisms governing these phenomena can be explained as follows:

(a) The initial state, without added salt (Fig. 11a**):** it was shown in Section 3.1.1. that divalent cations, in particular calcium and magnesium are predominant and account for about 80–95 % of the metals identified in *T. cordifolia* gum (Table 1). The condensation of these divalent cations on the anionic sites of the polyelectrolyte can lead either to the formation of inter- and intra-chain bridges through di-complexation (which would then lead to the collapse of the polyelectrolyte), or to a charge inversion. Charge inversion is the more likely scenario, given the excellent solubility of the gum in aqueous solution. The first scenario would be prevented by the large size of the divalent cations (atomic radii of Ca^{2+} and Mg^{2+} are 100 pm and 72 pm respectively as shown in Table A.1 **in Appendix A**) which would be greater than the distance between neighboring charges of the polyelectrolyte, preventing them from being inserted between two chains. This is all the more logical as the system has a high space occupancy with highly interpenetrated and tightly packed chains (as solutions are in the far-C** concentrated regime). Following charge inversion (with the exception of a few sites where monovalent cations are condensed), the polyelectrolyte behaves like a polycation in which repulsive interactions between charged groups of the same sign persist as illustrated in Fig. 11a.

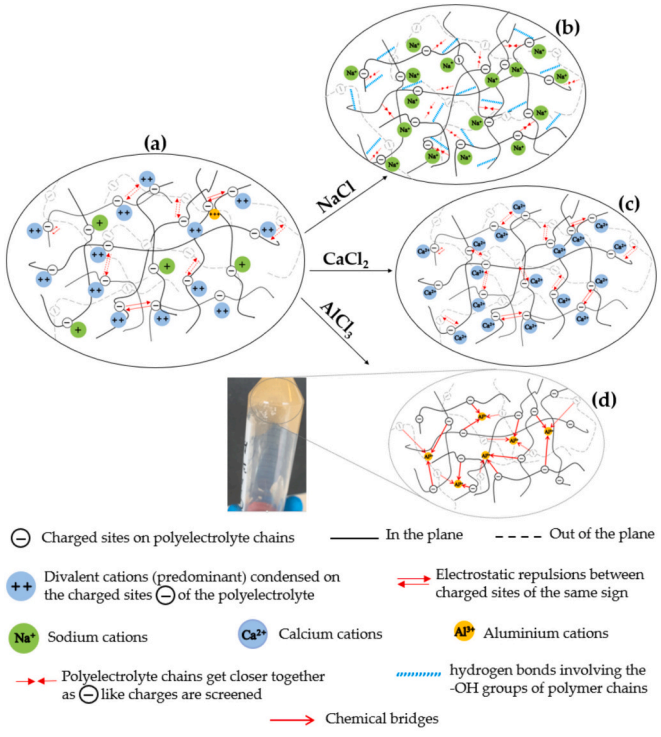

Fig. 11. Illustration of the mechanism governing the phenomena occurring in concentrated solutions of *T. cordifolia* gum (0.7 % *w*/w) when salts of different valences are added.

(b) In the presence of NaCl (Fig. 11b**):** competitive adsorption occurs between the added monovalent counter-ions and the divalent counter-ions initially present in the polyelectrolyte. According to Ermoshkin and de la Cruz [40] and Belloni et al. [41], electrostatic attractions favor the condensation of multivalent ions over monovalent ones, but an excess of monovalent ions is capable of reversing this trend by displacing multivalent ions. Therefore, it is likely that an excess of Na^+ ions led to the ejection of Ca^{2+} cations from the condensation sphere, giving rise to a succession of two effects: firstly, the addition of NaCl induces a screening of the electrostatic repulsions between the charged sites, and the system tends to collapse, with a consequent decrease in the viscosity of the solution as shown in Fig. 10a. Subsequently, as the polyelectrolyte shrinks, its chains move closer together, giving rise to associative interactions such as intermolecular hydrogen bonding (as illustrated in Fig. 11b), which increases their resistance to creep and flow, hence the observed increase in viscosity. A similar mechanism was proposed by Wyatt et al. [42] who also observed an increase in the zero-shear viscosity of concentrated solutions of several polyelectrolytes including xanthan, carrageenan and welan gums upon the addition of NaCl.

(c) In the presence of $CaCl_2$ (Fig. 11c**):** the added Ca^{2+} cations displace and substitute all the other counter-ions that were condensed on charged sites of the macro-ion. The polyelectrolyte thus becomes an integral polycation due to the total inversion of charges, and the repulsive interactions initially present within the system become accentuated (Fig. 11c), leading to the increase in viscosity. Above the threshold concentration of 0.1 M, the addition of $CaCl_2$ simply corresponds to the addition of free Ca^{2+} ions in the solution, with no significant impact on the condensation sphere. Belloni [43] predicted such a mechanism in which, beyond a certain threshold concentration, the number of condensed counter-ions remains constant and only the number of free counter-ions continues to increase.

(d) In the presence of $AlCl_3$ (Fig. 11d**):** divalent cations are ejected from the condensation sphere by trivalent Al^{3+} cations, whose interaction with the charged sites of the polyelectrolyte is stronger. Unlike Ca^{2+} cations which are quite bulky (ionic radius = 100 pm), the small ionic radius of Al^{3+} cations (r = 54 pm) makes them suitable for insertion between polyelectrolyte chains via a complexation mechanism (Table A.1). Indeed, according to Ermoshkin and de la Cruz [40], semi-dilute solutions of polyelectrolytes can form gels if the Bjerrum length and the distance between neighboring charged structural units along the chain are greater than the size of the ion. Menakbi et al. [54] have further shown that alginate gelation in the presence of trivalent cations, namely aluminum, occurs preferentially by complexation with three alginate chains involving three carboxylates per aluminum atom. Between neighboring charges in the same chain, di-complexation is possible but not tri-complexation, due to steric constraints. Tri-complexation therefore necessarily involves distant structural units, creating transverse intermolecular bridges that lead to a stiffer, more elastic three-dimensional network (high G'), resulting in gel formation as described in Fig. 11d. On the other hand, the syneresis and precipitation observed at higher concentrations of $AlCl_3$ could be linked to the hydrophobicity of the complexed sites due to dehydration of cations and polyelectrolyte as previously demonstrated by Sabbagh [44] and Sabbagh and Delsanti [45] with polyacrylate in the presence of multivalent cations. Furthermore, the non-redissolution of the precipitate (*T. cordifolia* gum-aluminum complex) when excess $AlCl_3$ is added, confirms the chemical signature between the Al^{3+} cations and the charged structural units (uronates) of *T. cordifolia* gum. Indeed, in the case of purely electrostatic associations, re-dissolution of the precipitate occurs at high concentrations of multivalent cations due to charge inversion and polyelectrolyte re-expansion [46,47].

3.2.3.2. Salt addition through dialysis. The interactions of the gum with added salts were further studied by using dialysis. To this end, a 0.2 % *w*/w *T. cordifolia* gum solution was dialyzed against several saline solutions at different concentrations namely 10^{-3}, 10^{-2}, 10^{-1} & 2×10^{-1} M for NaCl and $CaCl_2$; 10^{-4}, 5×10^{-4}, 10^{-3} & 5×10^{-3} M for $AlCl_3$ (the gum concentration was reduced to make the medium less viscous and ensure efficient ion exchange through the dialysis membrane). Under these conditions, at low salt concentrations (up to 10^{-3} M), the volume of solution inside the membranes remained visibly the same, whereas at higher concentrations (from 10^{-2} M for Na^+ and Ca^{2+} and from 5×10^{-3} M for Al^{3+}), the volume of solution inside the dialysis bags progressively decreased as the salt concentration increased, until complete dehydration for concentrations of the order of 10^{-1} M. These observations can be attributed to the salting-out phenomenon, during which the ions tend to strip the polyelectrolyte of solvent molecules (water). Initially, ions migrate from the dialysis solution (hypertonic) to the polyelectrolyte solution (hypotonic), tending towards isotonic equilibrium. Within the polyelectrolyte solution, there may be competitive reactivity between cations-polyelectrolyte and cations-solvent interactions.

The fact that salting-out is observed with monovalent and divalent cations as well as trivalent ones suggests that water ejection from the polyelectrolyte does not occur as a result of syneresis following gel formation, as observed with $AlCl_3$ in the previous section (since the monovalent salt is unable to establish intermolecular bridges). Therefore, the following mechanism can be proposed to explain the observations made in the case of dialysis: H^+ ions from the dialyzing solution would neutralize the negative charges of the polyelectrolyte, which would then change from -COO^- to -COOH, thus cancelling out electrostatic repulsions within the polyelectrolyte in favor of short-range attractive interactions such as hydrogen bonding, van der Waals interactions or even some hydrophobic interactions. These attractive polymer-polymer interactions would therefore be favored, while metal cations would preferentially interact with the solvent molecules (water), with which they would form small aqua complexes. Once transferred back into the dialysis solution through membrane exchange, as more water molecules are available, the small aqua complexes undergo successive complexations, and form large, fairly stable complexes of the type $M[H_2O]_n^{X+} \cdot mH_2O$, with $n + m = 5$–8, the octahedral $M[H_2O]_6^{x+}$ being favored [48,49] which then become too large to pass back through the membrane, hence the salting-out observed. Indeed, Ikeda et al. [50] demonstrated that for cations such as Ca^{2+}, water exchange reactions occur through an associative mechanism. With NaCl, about 1/4 of the water volume of the polyelectrolyte solution was ejected at 10^{-2} M, compared with 3/4 at the same concentration in $CaCl_2$ and 2/3 in the presence of 5×10^{-3} M $AlCl_3$. Subsequently, dialysis led to total water ejection for higher concentrations in the range of 2×10^{-1} M NaCl and 10^{-1} M $CaCl_2$, and to very thorough desiccation in the presence of 2×10^{-1} M $CaCl_2$. Thus, although salting-out occurs independently of the valency of the added salt, the above considerations suggest that the magnitude of salting-out would evolve in the order $Al^{3+} > Ca^{2+} > Na^+$, which follows a Hofmeister-like series, Al^{3+} being more kosmotropic (strongly hydrated) than Ca^{2+} and Na^+ [51]. This is consistent with the findings of Dragulet et al. [48] which revealed that the reactivity of these three metal cations with water follows the same order, sodium hydration shells being the least persistent.

For a better overview of the influence of the various parameters studied on the properties of *T. cordifolia* gum solutions, all the observations described above have been summarized in Table 4 below:

4. Conclusion

This work studied the rheological properties of aqueous *T cordifolia* gum solutions in the concentrated regime, including the effect of temperature, pH and added salts. Results revealed that the gum solution has a pseudoplastic fluid and weak-gel behavior. The gum solution is

Table 4
Comparative table of the influence of pH, temperature and added salts on the viscoelastic properties of *T. cordifolia* gum solutions.

Variables Effect on viscoelastic parameters	Temperature (20–80 °C)	pH	Added salts		
			NaCl	$CaCl_2$	$AlCl_3$
0.2 % (w/w)	**Observations** • **Thermostability** on heating (G′, G″ and tan δ unchanged) • O**ver-structuring** of the elastic contribution on cooling • No moduli crossover **Mechanism** Thermal agitation on heating — unfolding of associative groups — new intermolecular bridges on cooling— a more structured network.	/	**Observations** **Salting-out** (on dialysis) **Mechanism** Neutralization of COO^- by H^+ from dialysis solutions (electrostatic repulsion cancelled out) — attractive polymer-polymer interactions favored — cations-water molecules interactions favored — cation-aqua complexes outside the membrane and dehydrated polymer inside the membrane **Magnitude: $Al^{3+} > Ca^{2+} > Na^+$** (Hofmeister series)		
0.7 % (*w*/w)	**Observations** • **Perfect thermoreversibility** • No moduli crossover **Mechanism** Highly entangled system behaving like a rubber band: decrease in gel strength on heating (tan δ increases from 0.2 to 0.4) — **recovery of the initial structure** on cooling due to entropic forces (Brownian motion virtually absent in this case)	**Observations** • No significant change in viscosity for a moderate variation in pH (4.5–8); • Decrease in viscosity outside the intermediate pH range **Mechanism** Fluctuations in the acid-base balance of the carboxylic acid groups (uncharged at low pH, fully charged at high pH) — polymer collapse	**Observations** • **Decrease in viscosity** at low concentrations • **Increase in viscosity** at high concentrations **Mechanism** Condensation of Na^+ on COO^- — screening of electrostatic repulsions — the chains move closer together — intermolecular associations	**Observations** • **Moderate increase in viscosity** at low concentrations • **No change in viscosity** above a threshold concentration **Mechanism** Condensation of Ca^{2+} on COO^- — **total charge inversion** — strengthening of repulsive interactions — beyond a threshold concentration, added Ca^{2+} remain free in solution	**Observations** • **Gel formation** • **Exponential increase in viscosity** • **Increase in gel strength (decrease in tan δ)** • **Syneresis** and **precipitation** above a threshold concentration • No redissolution with an excess salt **Mechanism** Tricomplexation (**Al^{3+}-Uronate complexes**) favored by the small Al^{3+} cationic radius — transverse bridges within the system

frequency-dependent and has a very long relaxation time. Both shear and temperature induce associative interactions under certain conditions. The viscosity of concentrated solutions of *T. cordifolia* gum is less pH-dependent at intermediate values, but decreases considerably for lower and higher pH values. When salts are added, the viscoelastic response of the polyelectrolyte is strongly dependent on the valency and size of the salt, undergoing a screening charge effect with the monovalent, a charge inversion with the divalent, complexation giving rise to gelation with the trivalent salt, followed by syneresis as the concentration increases. Conversely, when salts are added through dialysis, the polyelectrolyte undergoes a salting-out regardless of the valency of the added salt. These interesting and complex results shed light on the mechanisms governing interactions within concentrated systems (under-researched) under various conditions, thereby establishing the link between structure and properties exhibited. They also inspire further work, including a more in-depth study of the observed antithixotropy, as well as the effect of salts under other conditions. Advanced structural analyses of the gum could also be ideal to better understand the structure-property relationships of *T cordifolia* gum.

CRediT authorship contribution statement

Michèle N. Fanwa: Writing – review & editing, Writing – original draft, Visualization, Validation, Methodology, Investigation, Funding acquisition, Conceptualization. **Nicolas Hucher:** Writing – review & editing, Validation, Supervision, Methodology, Conceptualization. **Arnaud M.Y. Cheumani:** Writing – review & editing, Validation, Project administration, Methodology, Conceptualization. **Maurice K. Ndikontar:** Writing – review & editing, Supervision, Funding acquisition. **Catherine Malhiac:** Writing – review & editing, Validation, Supervision, Methodology, Conceptualization. **Michel Grisel:** Writing – review & editing, Supervision, Project administration, Methodology, Funding acquisition, Conceptualization.

Declaration of competing interest

The authors declare that they have no known competing financial interests or personal relationships that could have appeared to influence the work reported in this paper.

Data availability

Data will be made available on request.

Acknowledgments

This work was supported by the SCAC (Service de Coopération et d'Action Culturelle), a French government scholarship. The author Michèle N. FANWA thanks the SCAC for the total financial coverage of her stay in France.

Appendix A

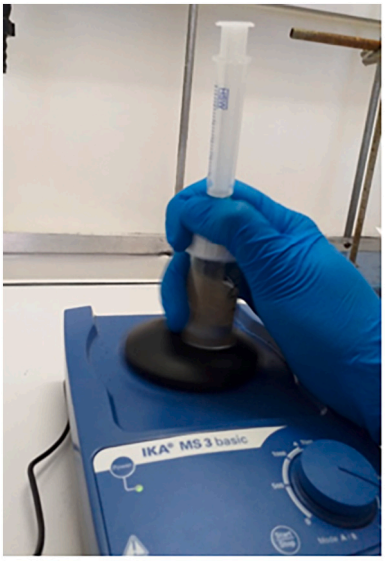

Fig. A.1. Addition of $AlCl_3$ salt to the 0.7 % *T. cordifolia gum* solution.

Table A.1
Ionic radii of cationic metals present in *T. cordifolia* gum [52,53].

Ion	Atomic radius (pm)
Na^+	102
Ca^{2+}	100
Mg^{2+}	72
Mn^{2+}	67
Fe^{2+}	61
Fe^{3+}	55
Al^{3+}	54
K^+	138
Zn^{2+}	74

References

[1] APG II, An update of the angiosperm phylogeny group classification for the orders and families of flowering plants: APG II, Bot. J. Linn. Soc. 141 (2003) 399–436, https://doi.org/10.1046/j.1095-8339.2003.t01-1-00158.x.

[2] R.B.T. Jiofack, Triumfetta cordifolia, in: M. Brink, E.G. Achigan-Dako (Eds.), Plant Resources of Tropical Africa 16. Fibres, PROTA Foundation/CTA, Wageningen, 2012, pp. 440–443.

[3] J.A. Carney, African traditional plant knowledge in the Circum-Caribbean region, J. Ethnobiol. 23 (2003) 167–185.

[4] K. Lay, The American species of *Triumfetta* L, Ann. Mo. Bot. Gard. 37 (1950) 317–318.

[5] B.L. Rye, A contribution to the taxonomy of the Tiliaceae of Western Australia, Nuytsia 9 (1994) 415–420.

[6] M.N. Fanwa, A.M.Y. Cheumani, B. Gügi, N. Hucher, C. Malhiac, M.K. Ndikontar, M. Grisel, Extraction, characterization and concentration regimes of the natural gum from *Triumfetta cordifolia* stem bark, Food Hydrocoll. 152 (2024) 109862, https://doi.org/10.1016/j.foodhyd.2024.109862.

[7] Saidou, C. (2012). Propriétés physico-chimiques et fonctionnelles des gommes hydrocolloïdes des écorces de *Triumfetta cordifolia* (Tiliacée) et de *Bridelia thermifolia* (Euphorbiacée). Doctoral thesis, Université de Grenoble, France. Retrieved from https://tel.archives-ouvertes.fr/tel-00870761.

[8] A.L. Woguia, J.L. Ngondi, T. Boudjeko, C. Rihouey, E.J. Oben, Hypolipidemic and antioxidative effects of Dika nut (*Irvingia gabonensis*) seeds and Nkui (*Trimphetta cordifolia*) stem bark mucilages in Triton WR-1339 induced hyperlipidemic rats, Food Sci. Biotechnol. 21 (2012) 1715–1721, https://doi.org/10.1007/s10068-012-0228-5.

[9] S. Chevassus-Agnes, J.C. Favier, A. Joseph, Technologie traditionnelle et valeur nutritive des «bières» de sorgho du Cameroun, ONAREST, Yaoundé, 1975.

[10] Ruffo, C. K., Birnie, A., & Tengnäs, B. (2002). *Edible wild plants of Tanzania*. RELMA (pp. 668–669).

[11] R.R. Schippers, *Triumfetta annua* L, in: G.J.H. Grubben, O.A. Denton (Eds.), Plant Resources of Tropical Africa 2. Vegetables, PROTA Foundation/Backhuys Publishers/CTA, Wageningen/Leiden/ Wageningen, 2004, pp. 535–537.

[12] M.N. Fanwa, C. Malhiac, N. Hucher, A.M.Y. Cheumani, M.K. Ndikontar, M. Grisel, *Triumfetta cordifolia* gum as a promising bio-ingredient to stabilize emulsions with potentials in cosmetics, Polymers 15 (2023) 2828, https://doi.org/10.3390/polym15132828.

[13] X. Li, Q. Yang, Y. Zhao, S. Long, J. Zheng, Dual physically crosslinked double network hydrogels with high toughness and self-healing properties, Soft Matter 13 (2017) 911–920, https://doi.org/10.1039/c6sm02567f.

[14] X. Callies, C. Véchambre, C. Fonteneau, S. Pensec, J. Chenal, L. Chazeau, L. Bouteiller, G. Ducouret, C. Creton, Linear rheology of supramolecular polymers center-functionalized with strong stickers, Macromolecules 48 (2015) 7320–7326, https://doi.org/10.1021/acs.macromol.5b01583.

[15] A. Susa, R.K. Bose, A.M. Grande, S. van der Zwaag, S.J. Garcia, Effect of the dianhydride/branched diamine ratio on the architecture and room temperature healing behavior of polyetherimides, ACS Appl. Mater. Interfaces 8 (2016) 34068–34079, https://doi.org/10.1021/acsami.6b10433.

[16] A. Susa, A. Mordvinkin, K. Saalwächter, S. van der Zwaag, S.J. García, Identifying the role of primary and secondary interactions on the mechanical properties and healing of densely branched polyimides, Macromolecules 51 (2018) 8333–8345, https://doi.org/10.1021/acs.macromol.8b01396.

[17] C. Teng, Y. Gao, X. Wang, W. Jiang, C. Zhang, R. Wang, D. Zhou, G. Xue, Reentanglement kinetics of freeze-dried polymers above the glass transition temperature, Macromolecules 45 (2012) 6648–6651, https://doi.org/10.1021/ma300885w.

[18] J.F. Vega, S. Rastogi, G.W.M. Peters, H.E.H. Meijer, Rheology and reptation of linear polymers. Ultrahigh molecular weight chain dynamics in the melt, J. Rheol. 48 (2004) 663–678, https://doi.org/10.1122/1.1718367.

[19] J. Lefebvre, J.-L. Doublier, Rheological behavior of polysaccharides aqueous systems, in: S. Dimitriu (Ed.), Polysaccharides: Structural Diversity and Functional Versatility, MarcelDekker, New York, 2005, pp. 357–394.

[20] H. Ramli, N. Zainal, M. Hess, C. Chan, Basic principle and good practices of rheology for polymers for teachers and beginners, Chem. Teach. Int. 4 (2022) 307–326, https://doi.org/10.1515/cti-2022-0010.

[21] M.S.M. Wee, Physico-Chemical Characterisation and Functionality of the Polysaccharide Extracted from the New Zealand Black Tree Fern, *Cyathea medullaris* (Mamaku), PhD. Thesis,, New Zealand, 2015.

[22] T.G. Mezger, Rhéologie Appliquée : Sur la route de la Rhéologie avec Joe Flow, 3rd ed., Graz, Autriche, Anton Paar GmbH, 2020, pp. 31–46.

[23] M.S.M. Wee, L. Matia-Merino, K.T.K. Goh, Time- and shear history-dependence of the rheological properties of a water-soluble extract from the fronds of the black tree fern, *Cyathea medullaris*, J. Rheol. 59 (2015) 365–376, https://doi.org/10.1122/1.4905006.

[24] L. Jin, Y. Shangguan, T. Ye, H. Yang, Q. An, Q. Zheng, Shear induced self-thickening in chitosan-grafted polyacrylamide aqueous solution, Soft Matter 9 (2013) 1835–1843, https://doi.org/10.1039/C2SM27404C.

[25] A.-L. Kjøniksen, M. Hiorth, J. Roots, B. Nyström, Shear-induced association and gelation of aqueous solutions of pectin, J. Phys. Chem. B 107 (2003) 6324–6328, https://doi.org/10.1021/jp0302358.

[26] A. Maleki, A.-L. Kjøniksen, B. Nyström, Anomalous viscosity behavior in aqueous solutions of hyaluronic acid, Polym. Bull. 59 (2007) 217–226, https://doi.org/10.1007/s00289-007-0760-2.

[27] De Couarraze, G., Grossiord, J.-L., & Huang, N. (2014). *Initiation à la rhéologie : Bases théoriques et applications expérimentales* (4ème ed.). Paris : Lavoisier (Chapitre 3).

[28] IUPAC, IUPAC compendium of chemical terminology version 2.3.3 2014-02-24, Retrieved from, https://goldbook.iupac.org/, 2014.

[29] A. Ponton, G. Ovarlez, Systèmes évolutifs, in: A. Ponton, J.-L. Grossiord (Eds.), La mesure en rhéologie: Des avancées récentes aux perspectives, EDP Sciences, Les Ulis, 2013, pp. 159–204, https://doi.org/10.1051/978-2-7598-1150-2.c010.

[30] G.A. Holzapfel, Nonlinear Solid Mechanics: A Continuum Approach for Engineering Science, John Wiley & Sons, West Sussex, 2000, p. 310.

[31] P.J. Veld, G.C. Rutledge, Temperature-dependent elasticity of a semicrystalline interphase composed of freely rotating chains, Macromolecules 36 (2003) 7358–7365, https://doi.org/10.1021/MA0346658.

[32] P. Mikulásek, R.J. Wakeman, J.Q. Marchant, The influence of pH and temperature on the rheology and stability of aqueous titanium dioxide dispersions, Chem. Eng. J. 67 (1997) 97–102, https://doi.org/10.1016/S1385-8947(97)00026-0.

[33] W.M. de Vos, S. Lindhoud, Overcharging and charge inversion: finding the correct explanation(s), Adv. Colloid Interf. Sci. 274 (2019) 102040, https://doi.org/10.1016/j.cis.2019.102040.

[34] M. Lukić, I. Pantelić, S.D. Savić, Towards optimal pH of the skin and topical formulations: from the current state of the art to tailored products, Cosmetics 8 (2021) 69, https://doi.org/10.3390/cosmetics8030069.

[35] S. Vázquez-Blanco, L. González-Freire, M.C. Dávila-Pousa, C. Crespo-Diz, pH determination as a quality standard for the elaboration of oral liquid compounding formula, Farm. Hosp. 42 (2018) 221–227, https://doi.org/10.7399/fh.10932.

[36] D.S. Anderson, The acid-base balance of the skin, Br. J. Dermatol. 63 (1951) 283–296, https://doi.org/10.1111/j.1365-2133.1951.tb13728.x.

[37] J.L. Du Plessis, A.B. Stefaniak, K.P. Wilhelm, Measurement of skin surface pH, Curr. Probl. Dermatol. 54 (2018) 19–25, https://doi.org/10.1159/000489514.

[38] R. Kohn, P. Kovac, Dissociation constants of D-galacturonic and D-glucuronic acid and their O-methyl derivatives, Chem. Zvesti 32 (1978) 478–485.

[39] A.V. Dobrynin, M. Rubinstein, Theory of polyelectrolytes in solutions and at surfaces, Prog. Polym. Sci. 30 (2005) 1049–1118, https://doi.org/10.1016/j.progpolymsci.2005.07.006.

[40] A.V. Ermoshkin, M.O. de la Cruz, Polyelectrolytes in the presence of multivalent ions: gelation versus segregation, Phys. Rev. Lett. 90 (2003) 125504, https://doi.org/10.1103/PhysRevLett.90.125504.

[41] L. Belloni, M. Drifford, P. Turq, Counterion diffusion in polyelectrolyte solutions, Chem. Phys. 83 (1984) 147–154, https://doi.org/10.1016/0301-0104(84)85229-5.

[42] N.B. Wyatt, C.M. Gunther, M.W. Liberatore, Increasing viscosity in entangled polyelectrolyte solutions by the addition of salt, Polymer 52 (2011) 2437–2444, https://doi.org/10.1016/j.polymer.2011.03.053.

[43] Belloni L. 1982. Interactions électrostatiques dans les solutions aqueuses de polyélectrolytes. Doctoral thesis, Université Pierre et Marie Curie Paris VI, France. Retrieved from https://inis.iaea.org/collection/NCLCollectionStore/_Public/45/085/45085827.pdf.

[44] Sabbagh, I. (1997). Stabilité de polymères anioniques en présence de cations multivalents. Doctoral thesis, Université Denis Diderot Paris VII, France. Retrieved from https://inis.iaea.org/collection/NCLCollectionStore/_Public/47/126/47126579.pdf.

[45] I. Sabbagh, M. Delsanti, Solubility of highly charged anionic polyelectrolytes in presence of multivalent cations: specific interaction effect, Eur. Phys. J. E: Soft Matter Biol. Phys. 1 (2000) 75–86, https://doi.org/10.1007/s101890050009.

[46] Esquenet, C. (2003). Propriétés structurales et dynamiques des solutions de polyélectrolytes rigides et semi-rigides et de polysaccharides associatifs. Doctoral thesis, Université Joseph Fourier, France. Retrieved from https://theses.hal.science/tel-00005468/document.

[47] J. Wittmer, A. Johner, J. Joanny, Precipitation of polyelectrolytes in the presence of multivalent salts, J. Phys. II 5 (1995) 635–654.

[48] F. Dragulet, A. Goyal, K. Ioannidou, R.J.-M. Pellenq, E. Del Gado, Ion specificity of confined ion–water structuring and nanoscale surface forces in clays, J. Phys. Chem. B 126 (2022) 4977–4989, https://doi.org/10.1021/acs.jpcb.2c01738.

[49] W. Grzybkowski, Nature and properties of metal cations in aqueous solutions, Pol. J. Environ. Stud. 15 (2006) 655–663.

[50] T. Ikeda, M. Boero, K. Terakura, Hydration properties of magnesium and calcium ions from constrained first principles molecular dynamics, J. Chem. Phys. 127 (2007) 074503, https://doi.org/10.1063/1.2768063.

[51] B.O. Myrvold, Salting-out and salting-in experiments with lignosulfonates (LSs), Holzforschung 67 (2013) 549–557, https://doi.org/10.1515/hf-2012-0163.

[52] D.R. Lide (Ed.), Handbook of Chemistry and Physics, 82nd ed., CRC Press, Boca Raton, 2001, pp. 1377–1771.

[53] H. Rollinson, J. Adetunji, Ionic radii, in: W.M. White (Ed.), Encyclopedia of Geochemistry. Encyclopedia of Earth Sciences Series, Springer, Cham, 2018, https://doi.org/10.1007/978-3-319-39312-4_340.

[54] C. Menakbi, F. Quignard, T. Mineva, Complexation of trivalent metal cations to mannuronate type alginate models from a density functional study, J. Phys. Chem. B. 120 (2016) 3615–3623, https://doi.org/10.1021/acs.jpcb.6b00472.